
Benchmark Example No. 33

# Work Laws in case of Fire for Concrete and Structural Steel

SOFiSTiK | 2024

**VERiFiCATiON**
**BE33 Work Laws in case of Fire for Concrete and Structural Steel**

VERiFiCATiON Manual, Service Pack 2024-4 Build 27



**SOFiSTiK AG**

HQ Nuremberg
Flataustraße 14
90411 Nürnberg
Germany

T +49 (0)911 39901-0
F +49(0)911 397904

Office Garching
Parkring 2
85748 Garching bei München
Germany

T +49 (0)89 315878-0
F +49 (0)89 315878-23

info@sofistik.com
www.sofistik.com



**Front Cover**

6th Street Viaduct, Los Angeles   Photo: Tobias Petschke

| Overview | |
|---|---|
| **Element Type(s):** | BF2D, SH3D |
| **Analysis Type(s):** | STAT, MNL |
| **Procedure(s):** | LSTP |
| **Topic(s):** | FIRE |
| **Module(s):** | TALPA, ASE |
| **Input file(s):** | temperature_compression.dat, quad_33.dat |

# 1 Problem Description

This benchmark is concerned with the validation of the structural analysis in case of fire with respect to the general calculation method according to DIN EN 1992-1-2. Therefore test case 5 is employed as presented in Annex CC of the standard DIN EN 1992-1-2/NA:2010-03 [1]. In this example the validation of the change in length of structural steel and concrete in compression, for the model of Fig. 1, at varying temperature and load capacity levels, is investigated.

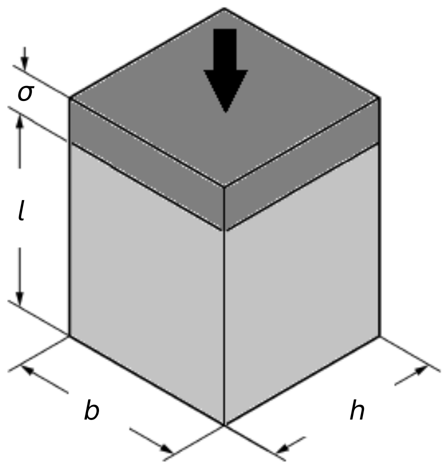


Figure 1: Problem Description

# 2 Reference Solution

The aim of Annex CC [1] is to check the applicability of the programs for engineering-based fire design on real structures. In this case the influence of the combination of increasing temperature and compressive loading with respect to the loading capacity of the structure is examined.

# 3 Model and Results

The properties of the model are defined in Table 1. A fictional beam as depicted in Fig. 1 is examined here, for the case of structural steel S 355 and of concrete C 20/25, with cross-sectional dimensions $b$ / $h$ = 10 / 10 $mm$, $l$ = 100 $mm$ and $b$ / $h$ = 31.6 / 31.6 $mm$, $l$ = 100 $mm$, respectively. Different temperatures and load levels are investigated. The boundary conditions are set such that stability failure is ruled out. The analysis is performed with TALPA, where the FIBER beam element is utilised. The computed and the reference results are presented in Table 2 for structural steel and in Table 3 for concrete. Fig. 2 presents stress-strain curves for structural steel for different temperature levels.

Table 1: Model Properties

| Material Properties | | Geometric Properties | | Test Properties |
|---|---|---|---|---|
| Steel | Concrete | Steel | Concrete | |
| S 355 | $C\ 20/25$ | $l = 100\,mm$ | $l = 100\,mm$ | Initial Conditions: |
| $f_{yk} = 355\,MPa$ | $f_{ck} = 20\,MPa$ | $h = 100\,mm$ | $h = 31.6\,mm$ | $\Theta = 20°C$ |
| Stress-strain: | Stress-strain: | $b = 10\,mm$ | $b = 31.6\,mm$ | Homog. temp.: |
| DIN EN 1993-1-2 | DIN EN 1992-1-2 | | | $20, 200, 400,$ |
| | | | | $600, 800°C$ |
| | | | | Loading: |
| | | | | $\sigma_{s(\Theta)}\ /\ f_{yk(\Theta)}$ |
| | | | | or |
| | | | | $\sigma_{c(\Theta)}\ /\ f_{ck(\Theta)} = 0.2, 0.6, 0.9$ |

Table 2: Results for Structural Steel - FIBER

| $\Theta$ [° $C$] | $\sigma_{s(\Theta)}\ /\ f_{yk(\Theta)}$ | Ref. [1] $\Delta l\ [mm]$ | SOF. $\Delta l'\ [mm]$ | $e_r$ [%] | Tol. [%] |
|---|---|---|---|---|---|
| 20 | 0.2 | 0.034 | 0.034 | 0.560 | |
| | 0.6 | 0.101 | 0.101 | −0.424 | |
| | 0.9 | 0.152 | 0.152 | −0.094 | |
| 200 | 0.2 | −0.194 | −0.194 | −0.141 | |
| | 0.6 | −0.119 | −0.119 | −0.119 | |
| | 0.9 | 0.159 | 0.156 | 1.794 | |
| 400 | 0.2 | −0.472 | −0.472 | 0.097 | |
| | 0.6 | −0.293 | −0.294 | −0.305 | ± 3 % |
| | 0.9 | 0.451 | 0.449 | 0.525 | |
| 600 | 0.2 | −0.789 | −0.789 | 0.053 | |
| | 0.6 | −0.581 | −0.581 | −0.054 | |
| | 0.9 | 0.162 | 0.160 | 1.245 | |
| 800 | 0.2 | −1.059 | −1.059 | 0.030 | |
| | 0.6 | −0.914 | −0.914 | −0.028 | |
| | 0.9 | −0.170 | −0.172 | −1.164 | |

Table 3: Results for Concrete - FIBER

| $\Theta$ [° $C$] | $\sigma_{s(\Theta)}$ / $f_{yk(\Theta)}$ | Ref. [1] $\Delta l$ [$mm$] | SOF. $\Delta l'$ [$mm$] | $e_r$ [%] | Tolerance [%] |
|---|---|---|---|---|---|
| 20 | 0.2 | 0.0334 | 0.0334 | 0.074 | |
| | 0.6 | 0.104 | 0.1036 | 0.428 | |
| | 0.9 | 0.176 | 0.1763 | −0.173 | |
| 200 | 0.2 | −0.107 | −0.1070 | 0.024 | |
| | 0.6 | 0.0474 | 0.0474 | −0.035 | |
| | 0.9 | 0.2075 | 0.2075 | 0.014 | |
| 400 | 0.2 | −0.356 | −0.3557 | 0.085 | |
| | 0.6 | −0.075 | −0.0750 | 0.016 | ± 3 % |
| | 0.9 | 0.216 | 0.2160 | −0.009 | |
| 600 | 0.2 | −0.685 | −0.6850 | −0.007 | |
| | 0.6 | 0.0167 | 0.0167 | −0.182 | |
| | 0.9 | 0.744 | 0.7442 | −0.033 | |
| 800 | 0.2 | −1.066 | −1.0662 | −0.023 | |
| | 0.6 | −0.365 | −0.3645 | 0.145 | |
| | 0.9 | 0.363 | 0.363 | −0.010 | |

Next step is the analysis of the same example with ASE where the QUAD element is now tested. The results are presented in Table 4 for structural steel and in Table 5 for concrete.

Table 4: Results for Structural Steel - QUAD

| $\Theta$ [° $C$] | $\sigma_{s(\Theta)}$ / $f_{yk(\Theta)}$ | Ref. [1] $\Delta l$ [$mm$] | SOF. $\Delta l'$ [$mm$] | $e_r$ [%] | Tolerance [%] |
|---|---|---|---|---|---|
| 20 | 0.2 | 0.034 | 0.034 | 0.560 | |
| | 0.6 | 0.101 | 0.101 | −0.424 | |
| | 0.9 | 0.152 | 0.152 | −0.094 | |
| 200 | 0.2 | −0.194 | −0.194 | −0.208 | |
| | 0.6 | −0.119 | −0.120 | −0.448 | |
| | 0.9 | 0.159 | 0.151 | 5.341 | |
| 400 | 0.2 | −0.472 | −0.472 | 0.010 | |
| | 0.6 | −0.293 | −0.297 | −1.447 | ± 3 % |
| | 0.9 | 0.451 | 0.422 | 6.396 | |
| 600 | 0.2 | −0.789 | −0.790 | −0.103 | |

Table 4: (continued)

| $\Theta$ [° $C$] | $\sigma_{s(\Theta)}$ / $f_{yk(\Theta)}$ | Ref. [1] $\Delta l$ [$mm$] | SOF. $\Delta l'$ [$mm$] | $e_r$ [%] | Tolerance [%] |
|---|---|---|---|---|---|
| | 0.6 | −0.581 | −0.589 | −1.302 | |
| | 0.9 | 0.162 | 0.130 | 19.626 | |
| 800 | 0.2 | −1.059 | −1.060 | −0.093 | |
| | 0.6 | −0.914 | −0.920 | −0.657 | |
| | 0.9 | −0.170 | −0.202 | −18.540 | |

Table 5: Results for Concrete - QUAD

| $\Theta$ [° $C$] | $\sigma_{s(\Theta)}$ / $f_{yk(\Theta)}$ | Ref. [1] $\Delta l$ [$mm$] | SOF. $\Delta l'$ [$mm$] | $e_r$ [%] | Tolerance [%] |
|---|---|---|---|---|---|
| 20 | 0.2 | 0.0334 | 0.0334 | 0.081 | |
| | 0.6 | 0.1040 | 0.1036 | 0.429 | |
| | 0.9 | 0.1760 | 0.1763 | −0.173 | |
| 200 | 0.2 | −0.1070 | −0.1070 | 0.019 | |
| | 0.6 | 0.0474 | 0.0474 | −0.037 | |
| | 0.9 | 0.2075 | 0.2075 | 0.015 | |
| 400 | 0.2 | −0.3560 | −0.3557 | 0.082 | |
| | 0.6 | −0.0750 | −0.0750 | 0.014 | ± 3 % |
| | 0.9 | 0.2160 | 0.2160 | −0.008 | |
| 600 | 0.2 | −0.6850 | −0.6851 | −0.010 | |
| | 0.6 | 0.0167 | 0.0167 | −0.207 | |
| | 0.9 | 0.7440 | 0.7442 | −0.033 | |
| 800 | 0.2 | −1.0660 | −1.0663 | −0.025 | |
| | 0.6 | −0.3650 | −0.3645 | 0.147 | |
| | 0.9 | 0.3631 | 0.3630 | −0.014 | |

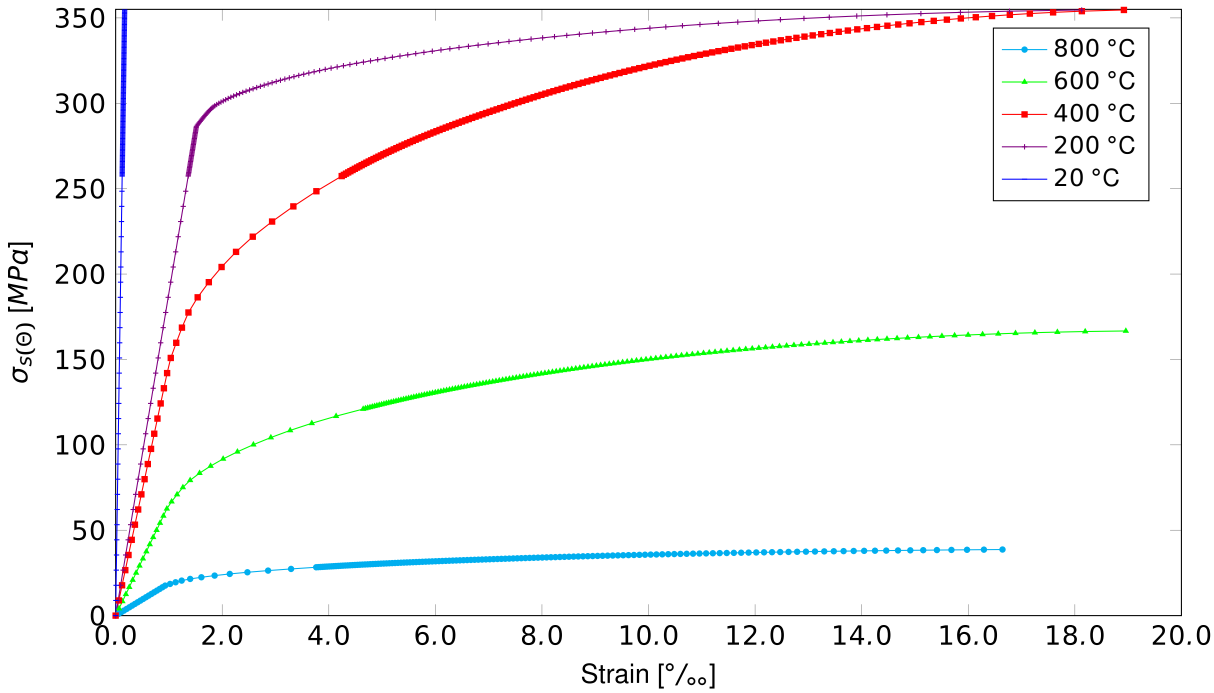


Figure 2: Steel Loading Strains

# 4 Conclusion

This example verifies the change in length of structural steel and concrete at different temperature and load levels. It has been shown that the calculation results with TALPA and the FIBER beam element are in very good agreement with the reference results. For the case of the QUAD layer element the results present some deviation only for the structural steel and specifically for the case of a high stress level, reaching the 90% of the steel strength.

# 5 Literature


[1] *DIN EN 1991-1-2/NA: Eurocode 1: Actions on structures, Part 1-2/NA: Actions on structures exposed to fire*. CEN. 2010.